ACS Sustainable Chemistry & Engineering

Research Article

pubs.acs.org/journal/ascecg

Facile Solution Dropping Method: A Green Process for Dyeing TiO_2 Electrodes of Dye-Sensitized Solar Cells with Enhanced Power Conversion Efficiency

Shih-Chieh Yeh,[†,‡] Pei-Heng Lee,[§] Hua-Yang Liao,[∥] Yu-You Chen,[†] Chin-Ti Chen,[*,†,§] Ru-Jong Jeng,[*,‡] and Jing-Jong Shuye[∥]

[†]Institute of Chemistry, Academia Sinica, 128, Academia Rd., Sec. 2, Taipei, Taiwan 11529, Republic of China

[‡]Institute of Polymer Science and Engineering, National Taiwan University, 1, Roosevelt Rd., Sec. 4, Taipei, Taiwan 10617, Republic of China

[§]Department of Applied Chemistry, National Chiao Tung University, 1001, University Rd., Hsinchu, Taiwan 30050, Republic of China

[∥]Research Center for Applied Sciences, Academia Sinica, 128, Academia Rd., Sec. 2, Taipei, Taiwan 11529, Republic of China

Supporting Information

ABSTRACT: A simple solution dropping method was established for sensitizing TiO_2 in the fabrication of dye-sensitized solar cells (DSCs). As compared with the conventional immersion dyeing process, this solution dropping method is very fast, taking less than ~5 min vs >5−10 h typically required in the traditional immersion dyeing process. There is much less organic solvent and dye substance (95% less) used in the dyeing TiO_2 process and hence significantly less disposal of chemical wastes from device fabrications. Therefore, this facile solution dropping method is a greener process than the immersion dyeing process. Moreover, the solution dropping method is superior to the immersion dyeing process in terms of power conversion efficiency (PCE) of the device. We have acquired compelling evidence through dye uptake assessment of TiO_2 electrodes, depth profile assay by SEM-EDX, and charge dynamic characteristics from transient photovoltage/photocurrent analysis indicating that the elevated dye loading level of a TiO_2 electrode is the main cause responsible for increasing short-circuit current and hence the PCE of DSCs. Three types of dye were used in this study to demonstrate the superiority of the solution dropping method, including classical **N719** (a ruthenium transition metal complex), **1P-PSS** (a metal free organic dye), and newly synthesized **ATT** (a β-pyrrole carbon-conjugated zinc tetraphenylporphyrin). Using the solution dropping method, dye uptake was improved from 3.0×10^{-7} to 9.9×10^{-7} mole cm^{-2}, 5.3×10^{-7} to 6.6×10^{-7} mole cm^{-2}, and 4.7×10^{-8} to 3.92×10^{-7} mole cm^{-2} for **N719**, **1P-PSS**, and **ATT**, respectively. In addition, the PCEs, averaged from 30 or 40 tested devices each with a 0.4 cm × 0.4 cm active area, were all improved from 8.1% to 8.5%, 5.9% to 6.6%, and 4.1% to 6.7% for **N719**, **1P-PSS**, and **ATT**, respectively.

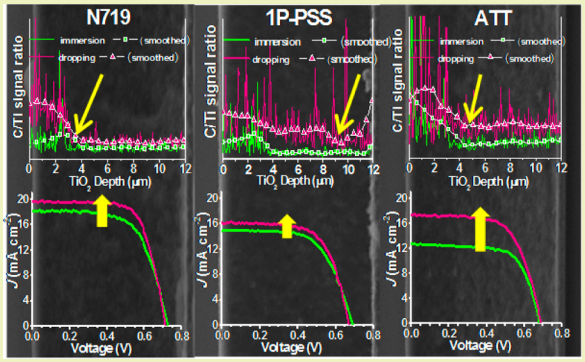

KEYWORDS: *Solution dropping method, Immersion dyeing process, Time saving, Material saving, Dye-sensitized solar cells (DSCs), Power conversion efficiency enhancing*

INTRODUCTION

One of the most intriguing solar energy technologies is probably dye-sensitized solar cells (DSCs), which is often referred to as the "Grätzel Cell" due to the inventor's namesake.[1,2] Nowadays, a power conversion efficiency (PCE) of as high as 13.15% has been achieved for the liquid electrolyte DSCs fabricated in a laboratory.[3] This remarkable achievement actually has come a long way after exploring numerous sensitizing dyes and optimizing countless nanoporous TiO_2 electrodes. The working principle of DSCs and various kinds of chemical sensitizers is well described by Hagfeldt et al. and Palomares et al.[4,5] In addition, many metal-free organic dyes were also summarized in the literatures reported by Harima et al. and Bäuerle et al.[6,7] Apart from that, further modification of nanoporous TiO_2 photoanodes has been demonstrated as an effective way to improve the performance of DSCs.[8−13] Development of better electrolyte systems is also indispensable in achieving high performance DSCs.[14−24] However, the so-called immersion dyeing process used in dyeing TiO_2 electrodes is a time-consuming process, commonly from 5 h

Received: August 25, 2014
Revised: November 6, 2014
Published: November 14, 2014

up to 16 h. Moreover, except for those improved dyeing processes (vide infra), most of the immersion dyeing processes generate a great amount of chemical wastes including organic solvents and dye substances. This makes such an innovated technology of producing renewable energy less attractive in practical manufacture due to the nature of the environmental hazards.

In the past decade, several improved TiO_2 dyeing methods have been developed.[25−29] These improved methods significantly shorten the time spent on the dyeing process. In one early case (a swift dye uptake procedure), the immersion dyeing process performed at elevated temperatures (∼50 °C) shortened the time of the TiO_2 dyeing process to less than 10 min.[28] However, the amount of chemical wastes generated from such a dyeing process remains as much as that as from the room temperature process. In fact, a similar TiO_2 dyeing method to the one investigated in ths study, that is, a solution "dropping" method, had been briefly mentioned, but no detailed follow-up study has been reported.[28] In other cases, chemicals used in the dyeing process have been significantly reduced by operation with the assistance from extra equipment or apparatus, which often incurs other problems, for example, an ultrafast dyeing process with the usage of an injection syringe to distribute dye solution onto a TiO_2 surface, of which the injection syringe is stationary with a fixed-point on the TiO_2 electrode.[25,26,29] In this improved dyeing process, the dye solution needs to diffuse through the whole surface area of the nanoporous TiO_2 structure. This injection method is able to drastically reduce the dyeing time to ∼2 min. However, dye substances are prone to precipitate (due to the insufficient solubility of most dye substances) during the diffusion, and aggregation or uneven dye distribution on TiO_2 tends to happen for such a stationary and fixed-point injection method. Another approach requires a "higee" system, which is a combination of spin coater and stainless sponge to homogenize the dispensed dye solution into fine droplets that "bombard" onto the TiO_2 electrode.[27] Similarly, clogging or precipitation of the dye substance inside a stainless sponge could cause problems, and maintenance (clean up) or replacement of the apparatus is necessary after each usage regardless of whether the same dye substance is used or not. Moreover, this spin-coating process still generates a considerable amount of chemical wastes, although the used dye solution is designed to be fully recycled. Just like the leftover dye solution from the conventional immersion dyeing process, it is hardly reusable due to the change of concentration and possible decomposition of the dye substance after the TiO_2 dyeing process, which is detrimental to the performance of fabricated DSCs.

As compared with either the temperature-elevated immersion dyeing process or fast dyeing methods mentioned above, the solution dropping method reported herein is an easier, greener (less chemical waste), and more reliable TiO_2 dyeing method. A very short period of time (5 min) and minimum dye solution (≤30 μL) are required in the solution dropping process of dyeing TiO_2 electrodes (with an active area of 0.4 cm × 0.4 cm). There is nearly no organic solvent waste or leftover dye substance from such a solution dropping method. Neither complicated equipment nor extra investment is needed. Moreover, low solubility dye substances, which are easily precipitated or aggregated inside the nanoporous TiO_2 electrode, are compatible with the solution dropping method, and hence, high PCEs are within reach. In this report, we demonstrate the success (saving time and materials and efficiency enhancement) of the solution dropping method with three kinds of dye substances, namely, **N719** (cis-bis(isothiocyanato)bis(2,2′-bipyridyl-4,4′-dicarboxylato) ruthenium(II) bis(tetrabutylammonium), **1P-PSS** ((*E*)-2-cyano-3-(5′-(5″-(p-(diphenylamino)phenyl)-thiophen-2″-yl)-thiophen-2′-yl)acrylic acid), and **ATT** (2-(thieno[3,2-*b*]-thiophene-2-acrylic acid)-5,10,15,20-tetraphenylporphinato zinc(II)) (Scheme 1).

Scheme 1. Chemical Structures of N719, 1P-PSS, and ATT

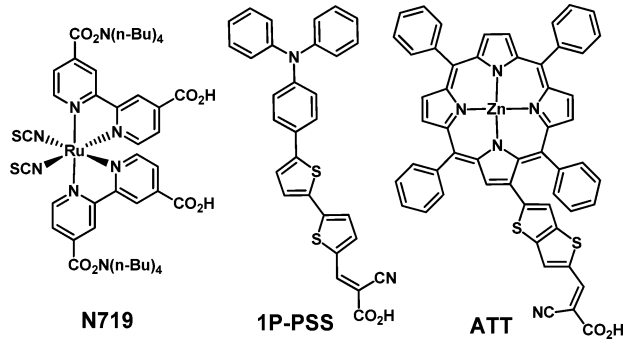

Quantitative examination of the dye uptake (by TiO_2 electrode) in the immersion dyeing and solution dropping methods was accomplished by UV−visible absorption spectroscopy (see Experimental Section for details). Energy-dispersive X-ray spectroscopy (EDX) from SEM line scans provided depth profile comparisons of the dye uptake inside TiO_2 electrodes between the immersion dyeing and solution dropping methods. Laser-pulsed transient photovoltage/photocurrent decay was utilized to investigate the charge dynamic properties of the immersion dyeing and solution dropping methods. Two kinds of TiO_2 electrodes were used in the present study. A TiO_2 electrode, 12T (12 μm transparent layer), was used for dye uptake measurement, SEM-EDX depth profile, and laser-pulsed transient photovoltage/photocurrent measurement, whereas 6T6S (6 μm transparent layer stacked with 6 μm scattering layer) was used for evaluating photovoltaic properties.

EXPERIMENTAL SECTION

Instrumentation of Structural Characterization of Photosensitizers. ^1H and ^{13}C NMR spectra were recorded on a Bruker AV400 MHz Fourier transform spectrometer at room temperature. UV−visible absorption spectra were recorded using a Hewlett-Packard 8453 absorption spectrometer. Elemental analysis was performed by an in-house service (Thermo Fisher Scientific FlashEA 1112) of the Institute of Chemistry. MALDI-TOF high resolution mass spectroscopy analysis (JMS-700 double focusing mass spectrometer) was performed by the Mass Spectrometry Laboratory of the Institute of Chemistry, Academia Sinica, Taiwan, ROC.

Materials Preparation and Synthesis. Materials for preparing electrolyte were purchased without further purification. Iodine (I_2), lithium iodide (LiI), and acetonitrile (AN) were purchased from Aldrich. 1-Butyl-3-methylimidazolium iodide (BMII) and 4-*tert*-butylpyridine (tBP) were purchased from TCI. The composition of the liquid electrolyte is I_2 (0.05M), LiI (0.1 M), BMII (0.6 M), and tBP (0.5 M) in acetonitrile. Co-absorbent chenodeoxycholic acid (CDCA) purchased from TCI was used in device fabrication as received. Two synthetic precursors, 2-(2-dioxolanyl)thieno[3,2-*b*]-thiophene (**1**) and 2-bromo-5,10,15,20-tetraphenyl porphyrin (**3**), were synthesized according to the procedures in literature.[30,31] Photosensitizer **N719** was purchased from Solaronix S.A., Switzerland. Metal-free organic dye **1P-PSS** was synthesized according to the

dx.doi.org/10.1021/sc500551e | *ACS Sustainable Chem. Eng.* 2015, 3, 71−81

Scheme 2. Synthesis Procedure of ATT

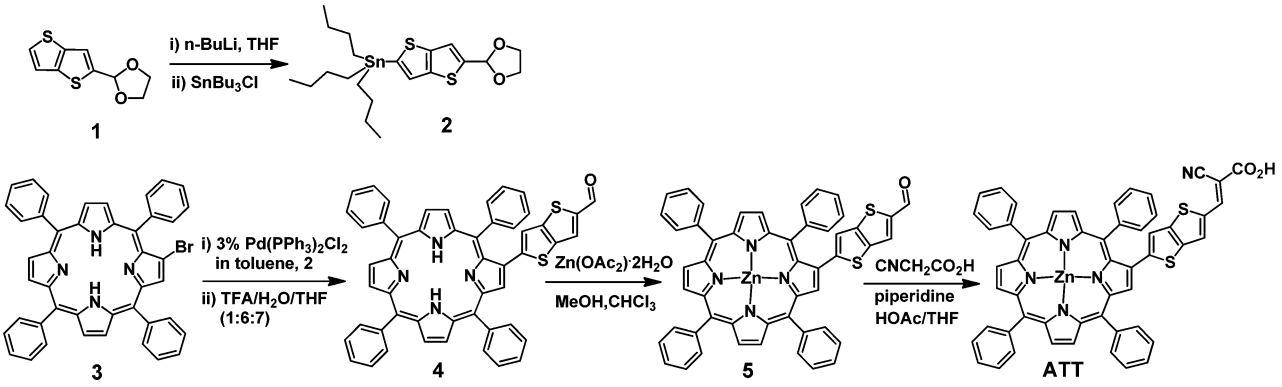

procedure reported in the literature.[32,33] The previously unknown porphyrin dye **ATT** was synthesized according to the procedures shown in Scheme 2.

*(5-(1,3-Dioxolan-2-yl)thieno[3,2-b]thiophen-2-yl)-tributylstannane (**2**).* **1** (2.14 g, 10 mmol) and 45 mL of THF were placed in a round-bottom flask under nitrogen atmosphere. After cooling the solution to −78 °C, 2.5 M *n*-butyllithium in hexanes (4.5 mL, 11.0 mmol) was added dropwise. The mixture was stirred for 1 h, and then tri-*n*-butyltin chloride (2.9 mL, 11 mmol) was added. The reaction mixture was warmed to room temperature and stirred for 16 h. The solution was extracted by ethyl acetate and saturated KF aqueous solution. After drying over magnesium sulfate, the solvent was removed under reduced pressure. The residual was subjected to flash column chromatography (triethylamine-treated silica gel, ethyl acetate/hexanes, 1/10). The product was isolated as a yellow viscous oil (note: right after purification, this product is unstable and requires low temperature storage as soon as possible) (2.94 g, 60%). ^{1}H NMR (400 MHz, $CDCl_3$): δ (ppm) 7.3 (s, 1H), 7.21 (s, 1H), 6.14 (s, 1H), 3.99−4.14 (m, 4H), 1.52−1.60 (m, 6H), 1.28−1.37 (m, 6H), 1.09−1.13 (m, 6H), 0.8−0.9 (t, J = 7.2 Hz, 9H). ^{13}C NMR (100 MHz, $CDCl_3$): δ (ppm) 144.07, 143.42, 141.60, 141.18, 126.76, 118.09, 100.64, 65.18, 28.81, 27.20, 13.59, 10.94. MALDI-TOF MS: calcd MW, 502.1022; m/e = 502.1041.

*2-(Thieno[3,2-b]thiophene-2-carboxaldehyde)-5,10,15,20-tetraphenylporphyrin (**4**).* To a 50 mL two-necked round-bottomed flask, **2** (0.39 g, 0.78 mmol), **3** (0.18 g, 0.26 mmol), $Pd(PPh_3)_2Cl_2$ (0.005 g, 0.007 mmol), and dry toluene (28 mL) were added under nitrogen atmosphere. The reaction was carried out at 95 °C for 48 h. After the removal of solvent, a solution of trifluoroacetic acid/H_2O/THF (2 mL/12 mL/14 mL) was added, and the resulting solution was stirred for 1 h. The solution was extracted with dichloromethane and saturated KF aqueous solution. The organic layers were collected and dried over magnesium sulfate. After the removal of solvent under reduced pressure, the residual was purified by flash column chromatography (silica gel) using dichloromethane/hexanes (v/v 1:1) as eluent. The desired product was isolated as a purple solid (0.12 g, 57%). ^{1}H NMR (400 MHz, $CDCl_3$): δ (ppm) 9.98 (s, 1H), 8.76−8.85 (m, 7H), 8.18−8.22 (m, 6H), 8.01 (d, J = 6.8 Hz, 2H), 7.88 (s, 1H), 7.72−7.76 (m, 8H), 6.75 (s, 1H), −2.64 (s, 2H). ^{13}C NMR (100 MHz, $CDCl_3$): δ (ppm) 183.33, 148.52, 146.51, 143.89, 142.12, 142.05, 141.68, 140.73, 138.31, 137.29, 135.21, 134.59, 134.54, 132.87, 132.63, 130.53, 129.76, 128.86, 127.93, 127.85, 126.84, 126.72, 126.05, 121.70, 120.97, 120.58, 120.49, 120.32. MALDI-TOF MS: calcd MW, 781.2096; m/e = 781.2115. Anal. calcd for $C_{51}H_{32}N_4OS_2$: C, 78.44; H, 4.13; N, 7.17. Found: C, 78.51; H, 4.63; N, 6.81.

*2-(Thieno[3,2-b]thiophene-2-carboxaldehyde)-5,10,15,20-tetraphenylporphinato zinc(II) (**5**).* To a stirred solution of 4 (0.1 g, 0.13 mmol) and chloroform (28 mL), $Zn(OAc)_2{\cdot}2H_2O$ (0.29 g, 1.3 mmol) dissolved in methanol (6 mL) was added. After refluxing for 4 h, the reaction mixture was extracted with chloroform and deionized water. The organic layers were then dried over magnesium sulfate, and the solvent was removed under reduced pressure. The mixture was purified by flash column chromatography (silica gel) using dichloromethane/hexanes (v/v 1:1) as eluent. The isolated solid was recrystallized from chloroform and methanol to afford a purple solid (0.09g, 85%). ^{1}H NMR (400 MHz, $CDCl_3$): δ (ppm) 9.99(s, 1H), 9.02 (s, 1H), 8.90−8.94 (m, 4H), 8.85 (d, J = 4.8 Hz, 1H), 8.80 (d, J = 4.8 Hz, 1H), 8.17−8.21 (m, 6H), 7.98 (d, J = 6.8 Hz, 2H), 7.88 (s, 1H), 7.71−7.75 (m, 8H), 6.78 (s, 1H). ^{13}C NMR (100 MHz, $CDCl_3$): δ (ppm) 183.13, 151.16, 150.90, 150.86, 150.84, 150.81, 150.25, 149.11, 146.87, 146.52, 145.78, 143.55, 143.35, 142.60, 141.53, 138.10, 136.98, 136.86, 134.89, 134.44, 133.00, 132.36, 131.77, 127.60, 126.60, 125.66, 121.91, 121.71, 121.65. MALDI-TOF MS: calcd MW, 842.1152; m/e = 842.1177. Anal. calcd for $C_{51}H_{30}N_4OS_2Zn$: C, 72.55; H, 3.58; N, 6.64. Found: C, 72.55; H, 3.83; N, 6.42.

*2-(Thieno[3,2-b]thiophene-2-acrylic acid)-5,10,15,20-Tetraphenylporphinato zinc(II) (**ATT**).* **5** (0.014 g, 0.016 mmol), 2-cyanoacetic acid (0.012 g, 0.133 mmol), and piperidine (0.04 mL, 0.397 mmol) were mixed in acetic acid/THF (2 mL/4 mL). The reaction mixture was stirred at 60 °C for 48 h and then poured into 100 mL deionized water. After standing for 24 h, the solid was separated by filtration and dried under vacuum to obtain a purple solid (0.010 g, 66%). ^{1}H NMR (400 MHz, $CDCl_3$): δ (ppm) 9.02 (s, 1H), 8.91−8.92 (m, 4H), 8.86 (d, J = 2.3 Hz, 1H), 8.80 (d, J = 2.3 Hz, 1H), 8.16−8.22 (m, 6H), 7.99 (d, J = 3.5 Hz, 2H), 7.91 (s, 1H), 7.68−7.81 (m, 8H), 6.96 (s, 1H), 6.75 (s, 1H), 6.54 (s, 1H). UV−vis (THF): λ_{max}/nm (ε, 10^3 $M^{-1}cm^{-1}$) = 430 (230), 522 (4.9), 562 (20.7), 602 (8.4). ^{13}C NMR (100 MHz, d_6-DMSO): δ (ppm) 163.68, 150.34, 149.88, 149.82, 149.25, 146.62, 145.99, 145,12, 144.89, 144.37, 142.50, 141.53, 137.68, 136.99, 135.84, 134.86, 134.13, 132.57, 131.88, 131.28, 129.13, 127.50, 127.11, 126.61, 126.52, 125.52, 121.98, 121.38, 120.67, 120.39, 118.22. MALDI-TOF MS: calcd MW, 909.1211; m/e = 909.1216. Anal. calcd for $C_{54}H_{31}N_5O_2S_2Zn{\cdot}4H_2O$: C, 65.95; H, 4.00; N, 7.12. Found: C, 66.51; H, 4.51; N, 6.21.

Preparation of TiO_2 FTO Electrodes and Pt Counter Electrodes. Procedures of preparing TiO_2 FTO (fluorine-doped tin oxide) electrodes and counter Pt-electrodes were modified based on those reported in the literature.[34] Double-layer nanoporous TiO_2 electrodes, composed of a transparent layer (T) and scattering layer (S), were prepared by applying pastes of TiO_2 (Solaronix) with two particle sizes (diameter of 15−20 and 400 nm, respectively) onto a FTO glass using a doctor blade technique. The electrodes were sintered at 500 °C for 30 min. Fabricated TiO_2 FTO was further modified by post-treatment of a 50 mM $TiCl_4$ solution ($TiCl_4$ + H_2O) in order to improve the connection of TiO_2 nanoparticles. Two types of TiO_2 FTO electrodes were fabricated in this work: 12T (12 μm transparent layer) TiO_2 electrodes for SEM EDX analysis and dye uptake evaluation and 12T and 6T6S (6 μm transparent +6 μm scattering layer) TiO_2 for DSCs fabrication. The 12T DSCs were for laser-pulsed transient photovoltage/photocurrent, whereas the 6T6S DSCs were for photovoltaic properties. The thickness of the TiO_2 electrode was determined by Veeco Detak 150 profilometer. The Pt counter electrode of DSC was prepared by dropping H_2PtCl_6 (Alfa Aesar) ethanol solution (4 mg H_2PtCl_6 in 1 mL ethanol) on FTO glass and then sintering at 400 °C for 10 min, and the process was repeated three times. The thicker Pt counter electrodes were used in this work.

dx.doi.org/10.1021/sc500551e | ACS Sustainable Chem. Eng. 2015, 3, 71−81

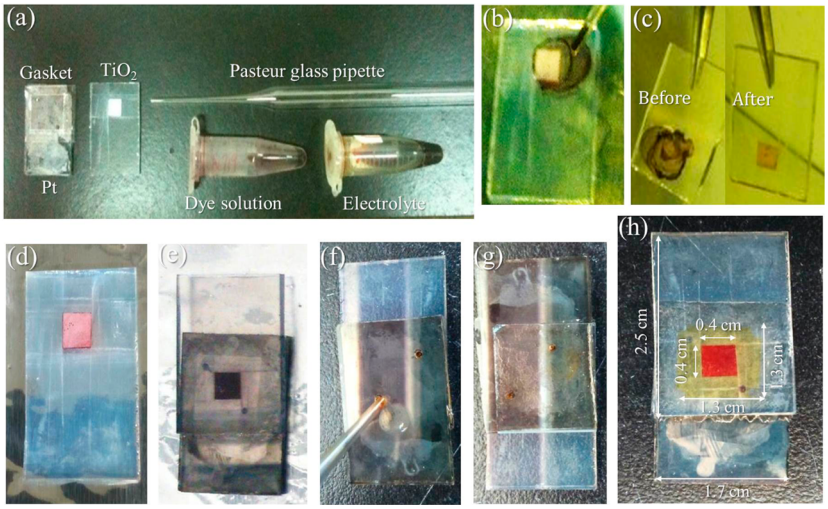

Figure 1. DSC fabrication using the solution dropping method in dyeing TiO_2 FTO electrodes: (a) materials and components, (b) dye solution dropped through Pasteur glass pipet to TiO_2 electrode, (c) heated (i.e., before) and rinsed (i.e., after) electrodes, (d) electrode after 120 °C thermal treatment, (e) assembled electrode and counter electrode, (f) assembled device with electrolyte injection, (g) sealing and packaging of the device, and (h) front view of the device.

For checking the conductive quality of the Pt counter electrodes, four-point probe equipment (Quatek Co., Ltd. CT5601Y) was used for resistance measurements in advance when the electrode was reused. We set a top limit resistance of 3 Ω sq^{-1} for the quality control of conductivity.

Dyeing TiO_2 FTO Electrode and Device Assembly. Two TiO_2 dyeing methods were used in this work to achieve high performance DSCs. For the conventional immersion dyeing process, TiO_2 electrodes were immersed into a 0.3 mM dye solution containing 10 mM chenodeoxycholic acid (CDCA) as the coabsorbent. For the immersion dyeing condition, the TiO_2 electrodes were immersed into dye solutions using a cosolvent of acetonitrile and *tert*-butyl alcohol (v/v; 1/1), cosolvent of methanol and THF (v/v; 1/1), and methanol, for **N719**, **1P-PSS**, and **ATT**, respectively. Devices for immersion time tests were 1 to 24 h, 1 to 16 h, and 5 to 240 min for **N719**, **1P-PSS**, and **ATT**, respectively. In addition, for evaluation of the multiple devices test, the immersion times were 24 h, 16 h, and 90 min for **N719**, **1P-PSS**, and **ATT**, respectively.

For the facile solution dropping method, the concentration of all dye solutions was 5 mM along with 10 mM CDCA. Methanol was used as solvent for **N719**, and **1P-PSS** was dissolved in a methanol/THF (v/v 1/1) cosolvent. **ATT** was dissolved in a methanol/DMSO (v/v 9/1) cosolvent. We simply used a Pasteur glass pipet as the dye solution dropping tool. Dosage of dye solution volume in the solution dropping method was in a range of 5−30 μL, calibrated by micropipette. To ensure sufficient dye-uptake during the dye solution dropping, the TiO_2 FTO electrode was heated directly on a hot plate (less than 2 min) at an elavated temperature of 60 °C for **N719** and **1P-PSS** and 60 or 145 °C for **ATT**.

All dyed TiO_2 electrodes were washed with 1−2 mL methanol or a cosolvent after the dyeing process and then heated at 120 °C (less than 1 min) for the removal of residual solvent. A Surlyn SX-1170-25 gasket (Solarnix) was used for sealing (120 °C and 1 min) the TiO_2 FTO electrode and Pt counter electrode together. It took less than 10 min to dye TiO_2 and gasket-seal the FTO and Pt electrodes in this solution dropping method. Taking the time for the injection of the liquid electrolyte into account, the fabrication of a single DSC usually could be completed within 15 min with this solution dropping method. Figure 1 photographically illustrates **N719**-based DSC fabrication using this method for dyeing TiO_2. The fabrication comprised eight steps all operated in ambient conditions. Figure 1a shows materials and components required for the process. The dye solution was first dropped through a Pasteur glass pipet to a TiO_2 electrode (Figure 1b). The electrode was heated on a hot plate and then rinsed with 1−2 mL dry methanol (Figure 1c). The electrode was further heated on a hot plate at 120 °C to remove residual solvent (Figure 1d). Subsquently, the TiO_2 electrode and Pt counter electrode were assembled with a gasket under thermal heating at 120 °C and mechanical pressure (Figure 1e), followed by injecting electrolyte into the assembled device (Figure 1f). The injection hole was then sealed and covered with glass, with further heating the device at 120 °C (Figure 1g). Figure 1h shows the front view of the device.

DSCs Photovoltaic Characterization. Controlled by a programmable source meter (Keithley 2400), the current density−voltage (J−V) characteristics of DSCs (without mask) was measured under AM 1.5G solar illumination from a class A solar simulator (Oriel 300 W). The light intensity was calibrated using a Si photodiode (PVM 172; area = 3.981 cm^2) from the National Renewable Energy Laboratory. The incident photon-to-current conversion efficiency (IPCE) of DSCs was measured in DC mode.[35] A Xe lamp as the light source was connected to a monochromator (Newport Model 74100) for selective wavelength output (by step of 10 nm) in a range of 300−800 nm. The intensity of each selected wavelength was in a range of 1 to 3 mW cm^{-2}. Measurements of photovoltaic parameters, short-circuit current (J_{SC}), open-circuit voltage (V_{OC}), and IPCE were carried out in ambient conditions. Fill factor (FF) and PCE of the device were calculated from the corresponding J−V curves.

Evaluation of Dye-Uptake of TiO_2 FTO Electrodes by UV−visible Absorption Spectroscopy. With UV−visible absorption spectrophotometer-determined dye solution concentration, we used eqs 1 and 2 to calculate the dye-uptake quantity (DU, in units of mole cm^{-2}) in the immersion dyeing and solution dropping method, respectively.

$$DU^{immersion} = [(C_1 - C_2) \times V_1]/[A_{TiO2}] \quad (1)$$

$$DU^{dropping} = [(C_3 \times V_2 - C_4 \times V_3]/[A_{TiO2}] \quad (2)$$

where $DU^{immersion}$ and $DU^{dropping}$ are dye-uptake (mol cm^{-2}) in the immersion dyeing and solution dropping method, respectively; C_1 (0.3 mM) and C_2 are the concentrations (mole L^{-1}) of the dye solution before and after the immersion dyeing process, respectively; V_1 is the volume (L) of the dye solution; A_{TiO2} is the surface area of 12T TiO_2 (area size 0.75 cm^2); C_3 (5 mM) and C_4 are the concentrations (mole L^{-1}) of the dye solution used in dropping method and dye solution collected from solvent rinsing of TiO_2 electrode after the dropping process, respectively; and V_2 and V_3 are the volume (L) of the dropping and rinsing solution, respectively. The extinction coefficient (ε) was predetermined by Beer's law, and the numbers were 11288, 14624, and 33420 M^{-1} cm^{-1} for **N719** (λ_{max} 530 nm in methanol), **1P-**

dx.doi.org/10.1021/sc500551e | ACS Sustainable Chem. Eng. 2015, 3, 71−81

PSS (λ_{max} 465 nm in methanol/THF v/v 1/1), and **ATT** (λ_{max} 560 nm in methanol), respectively.

Cross-Section SEM and EDX Analysis. Cross-section images of TiO_2 dye-uptake density and depth profiles were taken with a SEM (Nova200 NanoSEM, FEI Company, Hillsboro, OR, U.S.A.) operated at 7 kV. Because the speciments were insulators, a low vacuum detector was used, and the water pressure was fixed at 0.52 Torr. By using an energy dispersive spectrometer (IE450 X-Max80 silicon drift detector, Oxford Instrument, Abindgon, Oxfordshire, U.K.), the line profiles of elements C and Ti in the samples were presented.

Measurement of Transient Photovoltage and Photocurrent. Transient photovoltage (ΔV) and photocurrent (ΔQ) for charge dynamics studies were modified from those reported in the literature.[36−40] 12T TiO_2 DSCs (active area: 0.4 cm × 0.4 cm) were assembled with transparent Pt counter electrodes for preparing transparent DSCs. The preparation procedure was the same as the 6T6S DSCs. A tunable pulse laser (OPOTEK opoletteTM 355 I) was used as the excitation source (7 ns pulse width and 20 Hz repeating rate), and its wavelength and intensity were controlled by computer programming. Bias white light was supplied by a compact tungsten lamp, and the intensity was attenuated (fixed at 10 mW cm^{-2} in this work) by an absorptive neutral density filter set (Newport; FS-3R). The illumination of laser pulse (0.6 to 1.2 mJ cm^{-2}) was from the electrolyte electrode (EE) side for strong absorption.[37,38] On the basis of the most enhanced photocurrent wavelength observed in the IPCE spectra of the dye solution immersion and dropping fabrications, the illumination wavelengths of the laser pulse were 530, 500, and 550 nm for **N719**, **1P-PSS**, and **ATT**, respectively. The signals were recorded by a LeCory oscilloscope (model: LC547AM) averaging 100 sweeps, and the results were acquired by National Instruments GPIB USB-HS (1.8 MB/s). A programmable DC power supply (Sorensen HPD 60−5) was used as the bias voltage source for V_{OC}.

For transient photovoltage measurements, the cell was stabilized under bias white light for 15 s before the illumination of laser pulses. Photovoltage decay signals were monitored and recorded by an oscilloscope. Finally, the time constant was extracted from the dacaying signal by fitting with a single exponential. Transient photocurrent (at V_{OC}) was measured by applying a constant bias white light to the cell (10 mW cm^{-2}) under a contant voltage provided by a voltage source. The voltage source was set at the same voltage that counteracts the bias white light that generates in the open circuit condition, i.e., V_{OC}. The cell was also stabilized under bias white light for 15 s before the illumination by laser pulses. Similarly, the time constant was extracted from the dacaying signal by fitting with a single exponential.

RESULTS AND DISSCUSSION

Condition Optimization of Immersion and Dropping Methods for Dyeing TiO_2. In general, a long period of time is necessary for more dye-uptake by TiO_2 in the immersion dyeing process. However, a prolonged immersion dyeing process may not ensure effective increase of dye-uptake due to the adverse effect of dye aggregation. In order to have a fair comparison between the immersion dyeing process and solution dropping method, the dye solution immersion time and dosage of dye solution in the dropping method are examined in optimizing the device performance.

Ruthenium-based sensitizer **N719** is well known for DSCs with PCE as high as 9−10%.[41,42] Typically, in order to achieve better device performance, the optimized condition of immersion dyeing for **N719** is around 20−24 h with a solution concentration of 0.3 mM. As a matter of fact, our testing results indicated that a relative high J_{SC} could be obtained from the sample with a short time of immersion dyeing. Figure 2a shows the immersion time test for **N719** in this work, and the J_{SC} was higher than 17 mA cm^{-2} already after immersion for 2 h. The PCE went up to 8.15% with slightly increased J_{SC} of 17.6 mA

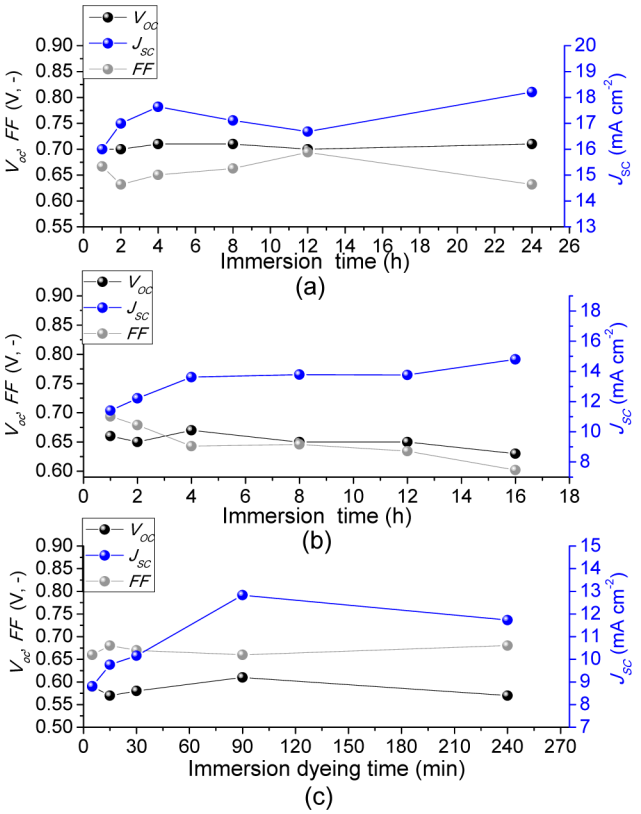

Figure 2. DSC performance (V_{OC}, FF, and J_{SC}) with various immersion time periods: DSCs with (a) **N719**, (b) **1P-PSS**, and (c) **ATT**.

cm^{-2} after immersion for 4 h. We found that the J_{SC} values of **N719** DSCs were in the range of 17−18.5 mA cm^{-2} for an immersion time of 4−24 h. These results for **N719** are very consistent with those from a recent report regarding the **N719** up-take issue studied by UV−visible absorption spectroscopy.[43] The equilibrium of adsorption and desorption of **N719** on TiO_2 would be reached more or less after 4 h of immersion dyeing time. As compared with those prepared at a shorter period of immersion time (the first 4 h), the increase in J_{SC} was moderate in a longer immersion time (beyond 12 h). On the other hand, the shortening of the immersion dyeing time (10−30 min) is possible with a high concentration of 20 mM, along with the addition of organic base (tetrabutylammonium hydroxide) in the immersion solution in order to increase the solubility of **N719**.[28] However, such a swift dyeing procedure is at the expense much of more dye substance (66 times more than that of regular concentration) and the usage of potential dye-harmful organic base in each immersion dyeing process, and hence, it is less practical and not commonly adopted in DSC fabrications. Accordingly, an immersion dyeing time period of 24 h is a better condition for **N719** in terms of maximizing PCEs and saving materials. When it comes to the optimized immersion dyeing time, the case for **1P-PSS** is rather similar to that for **N719** (Figure 2b). As long as the immersion dyeing time was more than 4 h, the PCE value of the **1P-PSS**-based device reached 5.2−5.8%. Longer immersion dyeing time could achieve a gain in J_{SC} (and PCE) further, although it was far less than the gain in the short immersion dyeing time (4 h). For the **1P-PSS**-based device with a long immersion dyeing time, the further gain in J_{SC} was largely offset by the steady decline of FF. Such declined FF was more pronounced in the

dx.doi.org/10.1021/sc500551e | ACS Sustainable Chem. Eng. 2015, 3, 71−81

case of **1P-PSS** (see Supporting Information for details). This is the cause of why the gain of PCE in the **1P-PSS**-based device was rather limited from a prolonged immersion dyeing process. Nevertheless, in order to be consistent with those reported in the literature,[32,33] we decided on 16 h as the ideal immersion dyeing time for the **1P-PSS** solution with a concentration of 0.3 mM. Within the context, it is very different for zinc porphyrin **ATT**. The newly synthesized **ATT** is less soluble in organic solvent and more prone to aggregate on the TiO_2 surface, that is, more sensitive to the nature of solvent and immersion time. Figure 2c shows the DSC performance test (J_{SC}, V_{OC}, and FF) for various immersion times of **ATT** (in methanol solution with concentrations of 0.3 mM and 10 mM for **ATT** and CDCA, respectively). For **ATT**-based DSCs, the optimized PCE of 5.3% was achieved at the immersion time of 90 min mostly because the highest J_{SC} (~12.8 mA cm^{-2}) could be reached at the moment. Beyond 90 min, the J_{SC} value decreased mainly due to **ATT** aggregation on the TiO_2 surface.

In addition to the dosage of the dropping dye solution, the temperature of the TiO_2 electrode used in the solution dropping process and solvent polarity (or eluting power of solvent) are some critical factors closely related to the performance of devices and the time length required by the solution dropping process. For speeding up solvent evaporation and shortening the process time of the solution dropping method, elevated substrate (TiO_2 electrode) temperatures, such as 60 °C for **N719** and **1P-PSS** and 60 or 145 °C for **ATT**, were used. However, the condition of elevated temperatures will limit the dye diffusion in TiO_2 due to fast solvent evaporation. Such adverse consequences can be largely overcome by using high polarity solvents for superior dye eluting power in TiO_2. In the solution dropping process, we used a mixed solvent of methanol and THF for **1P-PSS** and methanol for **N719** and **ATT**. In addition, the solvent with the higher polarity usually offers the possibility of carrying a higher concentration of the dyes. This is favorable for achieving a higher TiO_2 dye loading level with fewer drops of dye solution, that is, enhancing device performance and shortening the time for dyeing process. With CDCA (with a concentration of 10 mM) as the coabsorbent, the dropping dye solution with 5 mM concentration of **N719** or **1P-PSS** was prepared, whereas the solution with 1 mM concentration of **ATT** was prepared because of its relatively low solubility. Any dye remaining on the TiO_2 surface by physical adsorption was removed by solvent rinsing. Other factors, such as dropping solution dosage and TiO_2 substrate temperature, are potent variables enabling the optimization of saving time and materials in this dropping method. The results of the dropping dosage test are shown in Figure 3.

The J_{SC} value increased steadily as the dropping dosage increased with little or no decrease of V_{OC} and FF for the devices comprising any of these three dyes in the solution dropping fabrication. The high performance J_{SC} along with V_{OC} and FF means that the dye was well dispersive in the TiO_2 electrode even with a high dosage of dropping solution (25 μL for **N719** and **1P-PSS** and 90 μL for **ATT**). Through the solution dropping method, the photovoltaic parameters were J_{SC} = 18.2 mA cm^{-2}, V_{OC} = 0.7 V, FF = 0.62, and PCE = 7.9% for the **N719**-based device, J_{SC} = 17.6 mA cm^{-2}, V_{OC} = 0.65 V, FF = 0.62, and PCE = 7.1% for the **1P-PSS**-based device, and J_{SC} = 11.2 mA cm^{-2}, V_{OC} = 0.65 V, FF = 0.68, and PCE = 4.9% for **ATT**-based device. Particularly for the low solubility **ATT**, the usage of a mixed solvent methanol/DMSO (9/1 in volume ratio) for **ATT** in preparing the dropping solution (5 mM) would greatly improve the performance of fabricated DSCs (further performance comparison in the next section).

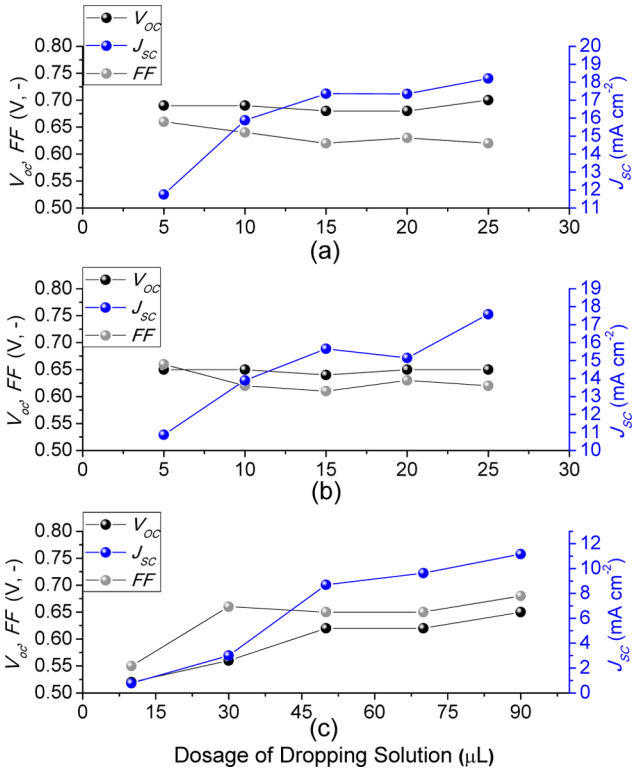

Figure 3. DSC performance (V_{OC}, FF, and J_{SC}) with various dosages of dropping solution: DSCs with (a) **N719**, (b) **1P-PSS**, and (c) **ATT**.

Between these two solution dyeing methods (immersion and dropping), the advantage of the solution dropping method is quite apparent. DSCs with higher J_{SC} values could be readily achieved with much a quicker dyeing process, and the dye consumption involved in the dyeing process is much less (about one tenth in each case).

Performance Comparison of DSCs Fabricated with Immersion Dyeing and Solution Dropping Methods. A total of 30 or 40 DSCs were fabricated based on each dye to investigate the performance reproducibility as well as for comparison for both the solution dropping method and immersion dyeing process. The immersion conditions for dyeing were 24 and 16 h for **N719** and **1P-PSS**, respectively, and 90 min for **ATT**. The concentration of all three immersion solutions was 0.3 mM. On the other hand, dosage of all three dropping solutions was 30 μL, and 5 mM was the concentration for all of them. In addition to the dye-uptake determined for both solution dyeing methods, the maximum, minimum, and mean value of photovoltaic parameters, such as J_{SC}, V_{OC}, FF, and PCE, are listed in Table 1. Figure 4 shows the photovoltaic performance for all of the samples.

The comparison of V_{OC} and FF between the samples by the immersion dyeing and solution dropping methods are plotted in the left of Figure 4. Although the mean value of V_{OC} or FF was virtually the same in case of **N719**- and **1P-PSS**-based devices, **ATT**-based DSCs exhibited a modest 50 mV higher V_{OC} by solution dropping than by immersion dyeing. Similar to those of **N719**- and **1P-PSS**-based devices, FF mean values of **ATT**-based DSCs showed little difference between the samples of the two solution dyeing methods. The comparison data of

dx.doi.org/10.1021/sc500551e | ACS Sustainable Chem. Eng. 2015, 3, 71−81

Table 1. Photovoltaic Parameters of DSCs and Dye-uptakes of TiO_2 Electrodes

device	method	J_{SC}^{avg} (min/max) (mA m^{-2})	V_{OC}^{avg} (min/max) (V)	FF^{avg} (min/max) (%)	PCE^{avg} (min/max) (%)	dye-uptake[c] (mol cm^{-2})
N719[a]	immersion	17.1 (16.1−18.8)	0.74 (0.72−0.76)	64 (57−69)	8.1 (7.2−8.9)	3.0×10^{-7}
	dropping	18.2 (16.5−19.8)	0.73 (0.71−0.76)	64 (57−70)	8.5 (7.7−9.8)	9.9×10^{-7}
1P-PSS[a]	immersion	14.4 (13.2−16.2)	0.65 (0.61−0.69)	63 (58−67)	5.9 (5.1−6.9)	5.3×10^{-7}
	dropping	15.2 (13.7−16.5)	0.67 (0.65−0.70)	65 (61−69)	6.6 (6.2−7.2)	6.6×10^{-7}
ATT[b]	immersion	11.0 (9.0−13.4)	0.61 (0.58−0.64)	62 (54−68)	4.1 (3.6−5.5)	4.7×10^{-8}
	dropping	16.6 (15.6−17.5)	0.66 (0.63−0.70)	63 (54−67)	6.7 (5.8−7.7)	3.2×10^{-7}

[a]Averages are taken from 30 devices, and the maximum/minimum values are included in parentheses. [b]A total of 30 and 40 devices of ATT fabricated with immersion dyeing and solution dropping methods, respectively. [c]Determined by UV−visible absorption spectroscopy on 12T TiO_2 FTO.

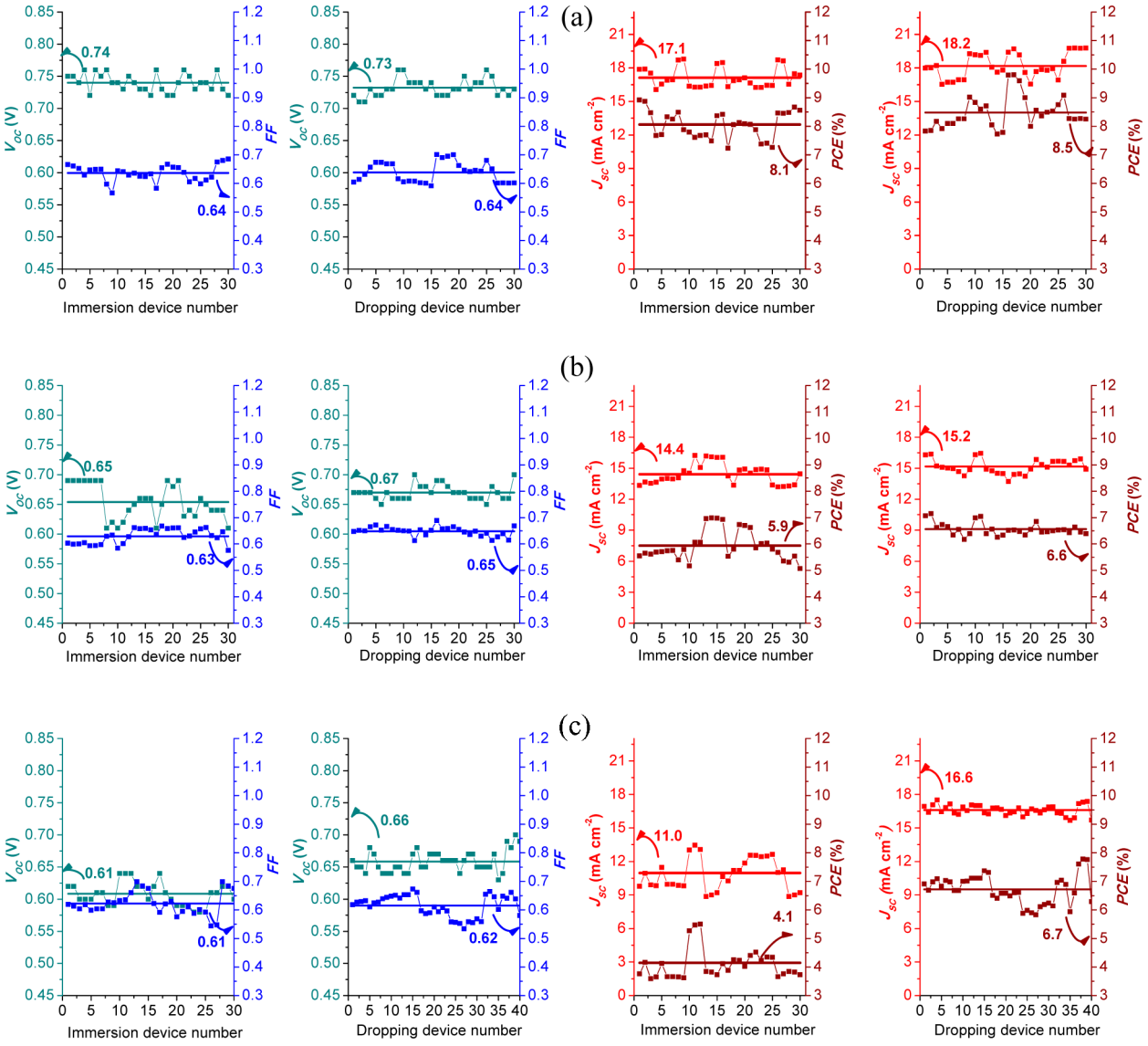

Figure 4. Comparison of photovoltaic performance of DSC fabricated with immersion dyeing and solution dropping methods: DSCs with (a) **N719**, (b) **1P-PSS**, and (c) **ATT**.

J_{SC} and PCE between the samples by the immersion dyeing and solution dropping methods are plotted in the right of Figure 4. From all the testing results of 30 or 40 DSCs, the advantage of the solution dropping method over the immersion dyeing process in achieving higher J_{SC} (and hence the correlated PCE) was obvious. Regarding the mean values of J_{SC}, they were 18.2 mA cm^{-2} vs 17.1 mA cm^{-2} for **N719**-based devices, 15.2 mA cm^{-2} vs 14.4 mA cm^{-2} for **1P-PSS**-based devices, and 16.6 mA cm^{-2} vs 11.0 mA cm^{-2} for **ATT**-based devices. Higher mean values of J_{SC} observed for DSCs are consistent with higher dye-uptake (dye loading level in TiO_2 electrode) values estimated for the samples prepared through the solution dropping method (Table 1). Regarding the mean values of PCE, they were 8.5% vs 8.1% for **N719**, 6.6% vs 5.9% for **1P-PSS**, and 6.7% vs 4.1% for **ATT**. For the samples prepared through the solution dropping method, the increase in J_{SC} was a major

dx.doi.org/10.1021/sc500551e | ACS Sustainable Chem. Eng. 2015, 3, 71−81

factor for enhancing PCE, which was in turn due to higher dye-uptake. Owing to the solution dropping method, the dye-uptakes exhibited a 3.3-, 1.25-, and 6.8-fold increase for **N719**-, **1P-PSS**-, and **ATT**-based devices, respectively. Among all DSCs, the **ATT**-based device possessed the largest improvement, 32.7% increase in J_{SC} and 63% increase in PCE, when the solution dropping method was utilized instead of the immersion process. Nevertheless, the enhancing ratio of J_{SC} was not proportional to the increased ratio of the dye loading level in all three cases. This could be attributed to the dye molecules diffusing much deeper into the TiO_2 electrode when the solution dropping method was utilized. Consequently, the incident light might be partially shielded due to the strong absorption of many dye molecules in "skin-deep" areas. Within the context, a higher TiO_2 dye-uptake is always associated with higher J_{SC} and PCE. Consequently, we could concur that the aggregation of dye molecules in the electrode via the solution dropping method was relatively modest. Perhaps, dye molecules were distributed more evenly and densely in the TiO_2 by the solution dropping method than immersion dyeing process. Accordingly, it is concluded that the dye molecules are forced farther down into the nanoporous TiO_2 electrode through the solution dropping method. Corresponding experimental evidence and further discussion will be provided in the next two sections.

Regarding the wavelength-dependent photocurrent output, Figure 5 shows IPCE spectra for the DSCs prepared via immersion and dropping methods. Various sizes of the yellowish shade in the figure indicate the difference of IPCE spectra between the devices prepared via the immersion and dropping method (**N719**-based device, Figure 5a, **1P-PSS**-based device, Figure 5b, and **ATT**-based device, Figure 5c). On the basis of different sizes of the yellowish shade, the increased ratios of IPCE were 8%, 6%, and 36% for **N719**-, **1P-PSS**-, and **ATT**-based devices, respectively. This is consistent with the increased ratios of J_{SC} measured for **N719**-, **1P-PSS**-, and **ATT**-based devices prepared from the solution dropping method, 6.4%, 5.6%, and 32.7%, accordingly. **ATT**-based DSCs exhibited rather different IPCE spectra, particularly in the visible region (475−625 nm) around the Q-band absorption. Apparently, the usage of the solution dropping method in dyeing TiO_2 led to more dye-uptake that improved light harvesting in the relevant wavelength region.

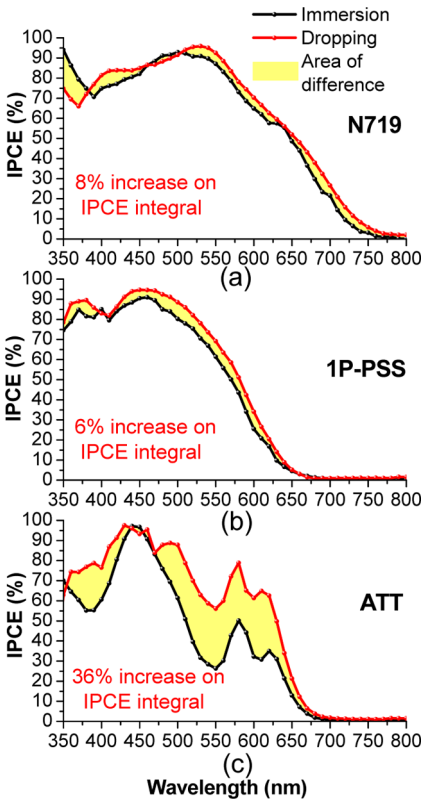

Figure 5. IPCE spectra of (a) **N719**-, (b) **1P-PSS**-, and (c) **ATT**-based DSCs.

Color Uniformity of Dyed TiO_2 Electrode and Its Depth Profile of SEM-EDX. On the basis of the photographs of dyed TiO_2 (6T6S FTO) with similar color intensity (Figure 6), each dye seemed to have similar distribution density on

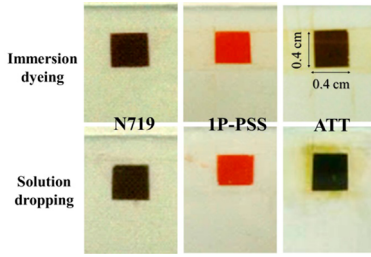

Figure 6. Photographs of **N719**-, **1P-PSS**-, and **ATT**-dyed TiO_2 from the immersion dyeing process and solution dropping method.

TiO_2 surface regardless of the methods used, either dropping or immersion. For both the solution dropping method and immersion dyeing process, color uniformity of the dyed TiO_2 electrode was sustained.

On the other hand, depth profile analysis of dyed TiO_2 electrodes (FTO coated with 12T) by energy-dispersive X-ray spectroscopy (EDX) provides insightful information about the dye in-depth distribution (Figure 7). First, according to the intensity of the carbon (C) signal from each dye substance, which is normalized with the titanium (Ti) signal in the same EDX measurement, the sample prepared from the solution dropping method exhibited higher signal intensity than that from the immersion dyeing process. Second, based on the C/Ti signal profile, the dye substance was distributed farther down into TiO_2-coated FTO for the sample by the solution dropping method. The **1P-PSS**-based electrode exhibited the deepest dye distribution, followed by the **ATT**-based electrode and then the **N719**-based electrode, accordingly. Such differences in in-depth distribution of each dye could be correlated to the chemical structure of the dye and solvents used in the solution dropping method. In addition to the characteristic of the bulky molecular shape, **N719** is the only dye bearing multiple TiO_2 anchoring groups (carboxylic acid or carboxylate), which greatly reduces the mobility of dye molecules in the TiO_2 matrix. On the other hand, the large molecular size of **ATT** is unfavorable for movement in the nanoporous TiO_2 matrix, but a less volatile and highly polar cosolvent dimethyl sulfoxide (DMSO) server could be an effective carrier medium in the TiO_2 matrix. This comes down to the most penetrating dye substance, **1P-PSS**, which can be attributed to the relatively small and linear molecular shape.

Investigation of Transient Photovoltage/Photocurrent. Laser-induced transient photovoltage (ΔV) and photo-

dx.doi.org/10.1021/sc500551e | *ACS Sustainable Chem. Eng.* 2015, 3, 71−81

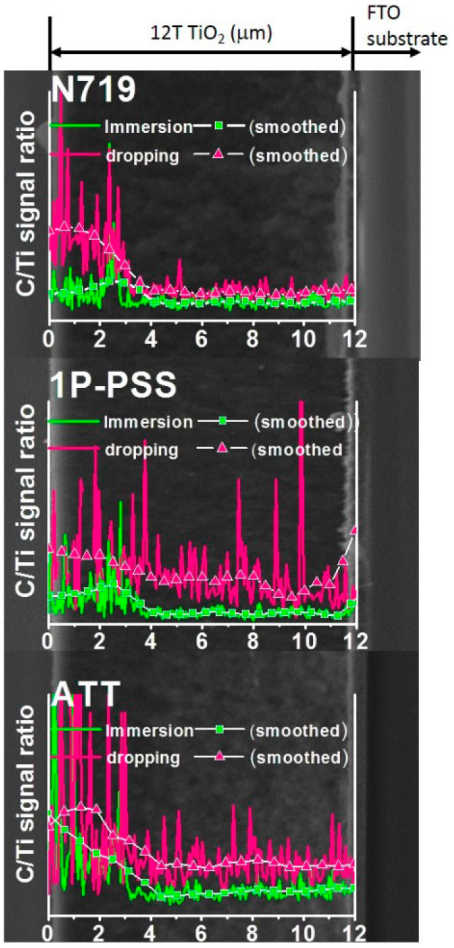

Figure 7. SEM cross-section images of TiO_2 (12T)-coated FTO and overlapped with depth traces of a EDX C/Ti signal acquired from the solution dropping method and immersion dyeing process. White symbol lines are the smoothened traces of the C/Ti EDX signal.

current (ΔQ) were performed to analyze the charge dynamic properties of those DSCs (see Experimental Section). The electron recombination lifetime (τ_e) and electron transport time (τ_{trans}) can be fitted to single exponential decay profile as shown in Figure 8. For the electron diffusion length (L) and diffusion coefficient (D_n), they are defined from equation $L = (D_n\tau_e)^{1/2} = (w^2\,\tau_e/2.35\,\tau_{trans})^{1/2}$, where w is the thickness of the TiO_2 electrode.[40] All the results acquired for DSCs prepared from both methods are listed in Table 2.

Table 2. Transient Photovoltage/Photocurrent of DSCs (Transparent 12T TiO_2 Electrode)

device[a]	method	τ_e[b] (ms)	τ_{trans}[c] (ms)	L[d] (10^{-4} cm)	D_n[d] (10^{-4} cm^2s^{-1})
N719	immersion	6.0	1.4	16	4.1
	dropping	10.0	1.1	24	5.6
1P-PSS	immersion	5.5	4.7	8	1.3
	dropping	6.5	2.9	12	2.1
ATT	immersion	7.4	1.9	15	3.2
	dropping	8.0	1.5	18	4.1

[a]Electrolyte: I_2 (0.05M), LiI (0.1 M), BMII (0.6 M), and tBP (0.5 M) in acetonitrile. [b]Fitted from photovoltage decay with single exponential. [c]Fitted from photocurrent decay with single exponential. [d]Calculated from $L = (D_n\tau_e)^{1/2} = (w^2\,\tau_e/2.35\,\tau_{trans})^{1/2}$.

All the acquired τ_e values of DSCs prepared from solution dropping were greater than those of DSCs from the immersion process, i.e., 10.0 ms > 6.0 ms, 6.5 ms > 5.5 ms, and 8.0 ms > 7.4 ms for **N719**-, **1P-PSS**-, and **ATT**-based devices, respectively. In contrast, all the acquired τ_{trans} values of DSCs from solution dropping were less than those of DSCs from the immersion process, i.e., 1.4 ms < 1.1 ms, 2.9 ms < 4.7 ms, and 1,2 ms < 1.3 ms for **N719**-, **1P-PSS**-, and **ATT**-based devices, respectively. The greater τ_e values of DSCs from solution dropping could be ascribed to the higher dye loading level (dye uptake) in TiO_2, which prevented the approach of I^-/I_3^- from electrolyte to TiO_2. Among which, the **N719**-based devices exhibited the most pronounced effect because the shallow dye

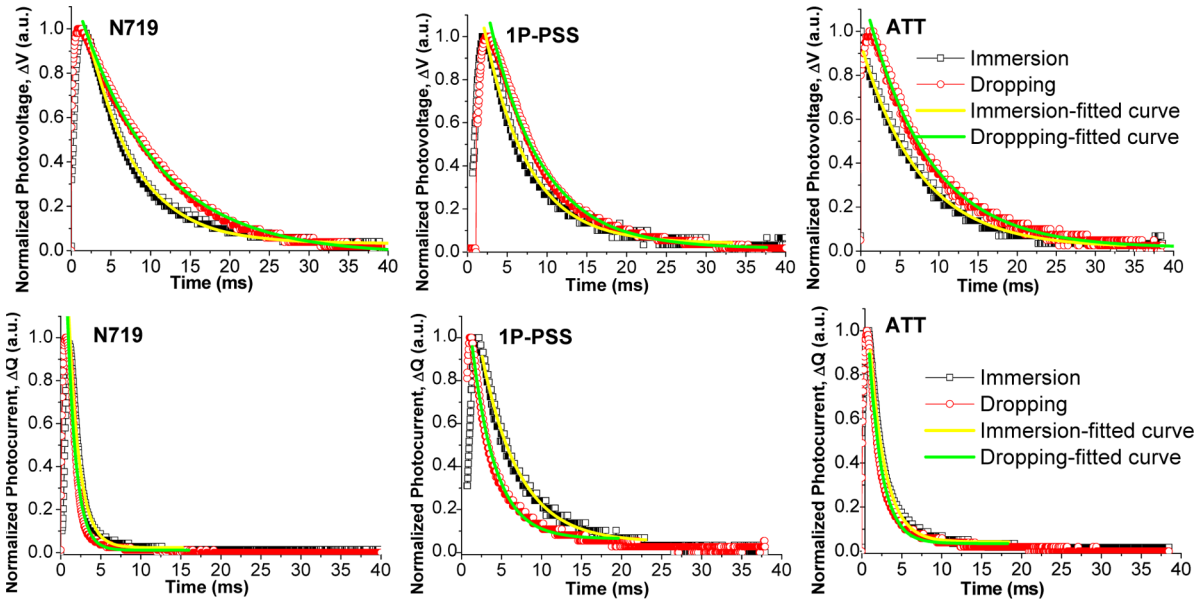

Figure 8. Transient photovoltage decay (top) and transient photocurrent decay (bottom) of DSCs.

dx.doi.org/10.1021/sc500551e | ACS Sustainable Chem. Eng. 2015, 3, 71−81

substance distribution was quite dense in the TiO_2 electrode. This is demonstrated by the depth profile study of SEM-EDX. Regarding τ_{trans}, more dye-loading content in the TiO_2 electrode is helpful in filling the trap state of TiO_2 and promoting electron transport (shorter τ_{trans}) from TiO_2 to FTO electrode. Among which, **1P-PSS**-based devices exhibited the most pronounced effect because of the deep distribution of **1P-PSS** in the TiO_2 electrode. This is also demonstrated by the depth profile study of SEM-EDX. Finally, the greater L and D_n estimated for DSCs fabricated with the solution dropping method indicate the presence of a higher charge collecting efficiency. This further corroborates the superiority of the solution dropping method in dyeing TiO_2 electrodes.

CONCLUSIONS

A facile solution dropping method was demonstrated for dyeing TiO_2 electrodes of DSCs. We have successfully illustrated the effectiveness of this method with three different dye substances, **N719**, **1P-PSS**, and **ATT**. As required by one of the reviewers, similar testing results of large size (0.5 cm × 2 cm) devices are provided in Figure S1 and Table S1 of the Supporting Information. The solution dropping method is a green process as compared with the conventional immersion dyeing process. This time-saving method requires much less chemical substance, particularly the organic solvent. Therefore, the method generates much less chemical waste, and hence, it is a better method for environment protection concern. Moreover, such a green process does not compromise the photovoltaic performance of DSCs. Due to the increased dye uptake (or dye loading level) in TiO_2, we have acquired convincing evidence to demonstrate that the enhanced PCE is mainly caused by the elevation of J_{SC}. Depth profile measurement by SEM-EDX delineates the dye distribution in the TiO_2 electrode. In-depth distribution of each dye is quite unique, dependent on chemical structure features. We also have conducted the measurement of transient photovoltage and photocurrent to provide an in-depth comparison of charge dynamics between DSCs prepared by the solution dropping method and immersion process. In addition, a PCE of 7.7% acquired for **ATT** DSCs in the present study is by far the highest among the β-carbon substituted (π-conjugated) zinc porphyrin.[44]

ASSOCIATED CONTENT

Supporting Information

Details of declining FF of 1P-PSS in solution dropping devices and esting results of large size DSCs (0.5 cm × 2 cm) from two dyeing methods. This material is available free of charge via the Internet at http://pubs.acs.org.

AUTHOR INFORMATION

Corresponding Authors

*(C.-T.C.) E-mail: chintchen@gate.sinica.edu.tw. Fax: +886 2 27831237. Tel: +886 2 27898542.

*(R.-J.J.) E-mail: rujong@ntu.edu.tw. Fax: +886 33665237. Tel: +886 2 33665884.

Notes

The authors declare no competing financial interest.

ACKNOWLEDGMENTS

This research was supported in part by the Ministry of Science and Technology of Taiwan, Academia Sinica, National Taiwan University, and National Chiao Tung University.

REFERENCES

(1) O'Regan, B.; Grätzel, M. A low cost, high efficiency solar cell based dye- sensitized colloidal TiO_2 films. *Nature* **1991**, *353*, 737−740.

(2) Peter, L. M. The Grätzel cell: Where next? *J. Phys. Chem. Lett.* **2011**, *2*, 1861−1867.

(3) Yella, A.; Mai, C. L.; Zakeeruddin, S. M.; Chang, S. N.; Hsieh, C. H.; Yeh, C. Y.; Grätzel, M. Molecular engineering of push−pull porphyrin dyes for highly efficient dye-sensitized solar cells: the role of benzene spacers. *Angew. Chem., Int. Ed.* **2014**, *53*, 2973−2977.

(4) Clifford, J. N.; Martinez-Ferrero, E.; Viterisi, A.; Palomares, E. Sensitizer molecular structure-device efficiency relationship in dye-sensitized solar cells. *Chem. Soc. Rev.* **2011**, *40*, 1635−1646.

(5) Hagfeldt, A.; Boschloo, B.; Sun, L.; Kloo, L.; Pettersson, H. Dye-sensitized solar cells. *Chem. Rev.* **2010**, *110*, 6595−6663.

(6) Mishra, A.; Fischer, M. K.; Bauerle, P. Metal-free organic dyes for dye-sensitized solar cells: From structure−property relationships to design rules. *Angew. Chem., Int. Ed.* **2009**, *48*, 2474−2499.

(7) Ooyama, Y.; Harima, Y. Molecular designs and syntheses of organic dyes for dye-sensitized solar cells. *Eur. J. Org. Chem.* **2009**, *2009*, 2903−2934.

(8) Dhas, V.; Muduli, S.; Agarkar, S.; Rana, A.; Hannoyer, B.; Banerjee, R.; Ogale, S. Enhanced DSSC performance with high surface area thin anatase TiO_2 nanoleaves. *Sol. Energy* **2011**, *85*, 1213−1219.

(9) Kim, B.; Park, S. W.; Kim, J. Y.; Yoo, K.; Lee, J. A.; Lee, M. W.; Lee, D. K.; Kim, J. Y.; Kim, B.; Kim, H.; Han, S.; Son, H. J.; Ko, M. J. Rapid dye adsorption via surface modification of TiO_2 photoanodes for dye-sensitized solar cells. *ACS Appl. Mater. Interfaces* **2013**, *5*, 5201−5207.

(10) Lee, C. P.; Chen, P. Y.; Vittal, R.; Ho, K. C. Enhanced performance of a dye-sensitized solar cell with the incorporation of titanium carbide in the TiO_2 matrix. *Phys. Chem. Chem. Phys.* **2010**, *12*, 9249−9255.

(11) Ramasamy, P.; Kang, M.-S.; Cha, H.-J.; Kim, J. Highly efficient dye-sensitized solar cells based on HfO_2 modified TiO_2 electrodes. *Mater. Res. Bull.* **2013**, *48*, 79−83.

(12) Tian, H.; Hu, L.; Zhang, C.; Chen, S.; Sheng, J.; Mo, L.; Liu, W.; Dai, S. Enhanced photovoltaic performance of dye-sensitized solar cells using a highly crystallized mesoporous TiO_2 electrode modified by boron doping. *J. Mater. Chem.* **2011**, *21*, 863−868.

(13) Zhang, X.; Thavasi, V.; Mhaisalkar, S. G.; Ramakrishna, S. Novel hollow mesoporous 1D TiO_2 nanofibers as photovoltaic and photocatalytic materials. *Nanoscale* **2012**, *4*, 1707−1716.

(14) Bai, Y.; Zhang, J.; Zhou, D.; Wang, Y.; Zhang, M.; Wang, P. Engineering organic sensitizers for iodine-free dye-sensitized solar cells: red-shifted current response concomitant with attenuated charge recombination. *J. Am. Chem. Soc.* **2011**, *133*, 11442−11445.

(15) Feldt, S. M. G.; Gabrielsson, E. A.; Sun, E.; Boschloo, L.; Hagfeldt, G. A. Design of organic dyes and cobalt polypyridine redox mediators for high-efficiency dye-sensitized solar cells. *J. Am. Chem. Soc.* **2010**, *132*, 16714−16724.

(16) Kashif, M. K.; Axelson, J. C.; Duffy, N. W.; Forsyth, C. M.; Chang, C. J.; Long, J. R.; Spiccia, L.; Bach, U. A new direction in dye-sensitized solar cells redox mediator development: in situ fine-tuning of the cobalt(II)/(III) redox potential through Lewis base interactions. *J. Am. Chem. Soc.* **2012**, *134*, 16646−16653.

(17) Klahr, B. M. H.; T, W. Performance enhancement and limitations of cobalt bipyridyl redox shuttles in dye-sensitized solar cells. *J. Phys. Chem. C* **2009**, *113*, 14040−14045.

(18) Kuang, D.; Wang, P.; Ito, S.; Zakeeruddin, S. M.; Grätzel, M. Stable mesoscopic dye-sensitized solar cells based on tetracyanoborate ionic liquid electrolyte. *J. Am. Chem. Soc.* **2006**, *128*, 7732−7733.

(19) Nusbaumer, H.; Zakeeruddin, S. M.; Moser, J. E.; Grätzel, M. An alternative efficient redox couple for the dye-sensitized solar cell system. *Chem.—Eur. J.* **2003**, *9*, 3756−3763.

(20) Sapp, S. A. E.; C, M.; Contado, C.; Caramori, S.; Bignozzi, C. A. Substituted polypyridine complexes of cobalt(II/III) as efficient electron-transfer mediators in dye-sensitized solar cells. *J. Am. Chem. Soc.* **2002**, *124*, 11215−11222.

(21) Tian, H.; Yu, Z.; Hagfeldt, A.; Kloo, L.; Sun, L. Organic redox couples and organic counter electrode for efficient organic dye-sensitized solar cells. *J. Am. Chem. Soc.* **2011**, *133*, 9413−9422.
(22) Tsao, H. N.; Yi, C.; Moehl, T.; Yum, J. H.; Zakeeruddin, S. M.; Nazeeruddin, M. K.; Grätzel, M. Cyclopentadithiophene bridged donor−acceptor dyes achieve high power conversion efficiencies in dye-sensitized solar cells based on the tris-cobalt bipyridine redox couple. *ChemSusChem* **2011**, *4*, 591−594.
(23) Yella, A.; Lee, H. W.; Tsao, H. N.; Yi, C.; Chandiran, A. K.; Nazeeruddin, M. K.; Diau, E. W.; Yeh, C. Y.; Zakeeruddin, S. M.; Grätzel, M. Porphyrin-sensitized solar cells with cobalt (II/III)-based redox electrolyte exceed 12% efficiency. *Science* **2011**, *334*, 629−634.
(24) Yoshida, Y.; Muroi, K.; Otsuka, A.; Saito, G.; Takahashi, M.; Yoko, T. 1-Ethyl-3-methylimidazolium based ionic liquids containing cyano groups: Synthesis, characterization, and crystal structure. *Inorg. Chem.* **2004**, *43*, 1458−1462.
(25) Holliman, P. J.; Davies, M. L.; Connell, A.; Vaca Velasco, B.; Watson, T. M. Ultra-fast dye sensitisation and co-sensitisation for dye-sensitized solar cells. *Chem. Commun.* **2010**, *46*, 7256−72588.
(26) Holliman, P. J.; Mohsen, M.; Connell, A.; Davies, M. L.; Al-Salihi, K.; Pitak, M. B.; Tizzard, G. J.; Coles, S. J.; Harrington, R. W.; Clegg, W.; Serpa, C.; Fontes, O. H.; Charbonneau, C.; Carnie, M. J. Ultra-fast co-sensitization and tri-sensitization of dye-sensitized solar cells with N719, SQ1 and triarylamine dyes. *J. Mater. Chem.* **2012**, *22*, 13318−13327.
(27) Kuo, H.-P.; Wu, C.-T. Speed up dye-sensitized solar cell fabrication by rapid dye solution droplets bombardment. *Sol. Energy Mater. Sol. Cells.* **2014**, *120*, 81−86.
(28) Nazeeruddin, M. K.; Splivallo, R.; Liska, P.; Comte, P.; Grätzel, M. A swift dye uptake procedure for dye-sensitized solar cells. *Chem. Commun.* **2003**, *12*, 1456−1457.
(29) Davies, M. L.; Watson, T. M.; Holliman, P. J.; Connell, A.; Worsley, D. A. In situ monitoring and optimization of room temperature ultra-fast sensitization for dye-sensitized solar cells. *Chem. Commun.* **2014**, *50*, 12512−12514.
(30) Prugh, J. D.; H, G. D.; Mallorga, P. J.; McKeever, B. M.; Michelson, S. R.; Murcko, M. A.; Schwam, H.; Smith, R. L.; Sondey, J. M.; Springer, J. P.; Sugrue, M. F. New isomeric classes of topically active ocular hypotensive carbonic anhydrase inhibitors: 5-Substituted thieno[2,3-b]thiophene-2-sulfonamides and 5-Substituted thieno[3,2-b]thiophene-2-sulfonamides. *J. Med. Chem.* **1991**, *34*, 1805−1808.
(31) Gao, G. Y.; R, J. V.; Allen, D. B.; Chen, Y.; Zhang, X. P. Synthesis of β-functionalized porphyrins via palladium-catalyzed carbon-heteroatom bond formations: expedient entry into β-chiral porphyrins. *J. Org. Chem.* **2007**, *72*, 9060−9066.
(32) Chang, Y. J.; Chow, T. J. Dye-sensitized solar cell utilizing organic dyads containing triarylene conjugates. *Tetrahedron* **2009**, *65*, 4726−4734.
(33) Thomas, K. R. J.; Hsu, Y.-C.; Lin, J.-T.; Lee, K.-M.; Ho, K.-C.; Lai, C.-H.; Cheng, Y.-M.; Chou, P.-T. 2,3-Disubstituted thiophene-based organic dyes for solar cells. *Chem. Mater.* **2008**, *20*, 1830−1840.
(34) Ito, S.; Murakami, T. N.; Comte, P.; Liska, P.; Grätzel, C.; Nazeeruddin, M. K.; Grätzel, M. Fabrication of thin film dye-sensitized solar cells with solar to electric power conversion efficiency over 10%. *Thin Solid Films* **2008**, *516*, 4613−4619.
(35) Sommeling, P. M.; R, H. C.; Roosmalen, J.A.M. van; Schonecker, A.; Kroon, J. M.; Wienke, J. A.; Hinsch, A. Spectral response and IV-characterization of dye-sensitized nanocrystalline TiO_2 solar cells. *Sol. Energy Mater. Sol. Cells.* **2000**, *62*, 399−410.
(36) Barnes, P. R.; Miettunen, K.; Li, X.; Anderson, A. Y.; Bessho, T.; Gratzel, M.; O'Regan, B. C. Interpretation of optoelectronic transient and charge extraction measurements in dye-sensitized solar cells. *Adv. Mater.* **2013**, *25*, 1881−1922.
(37) Kopidakis, N.; Benkstein, K. D.; L van de Lagemaat, J.; Frank, A. J. Transport-limited recombination of photocarriers in dye-sensitized nanocrystalline TiO_2 solar cells. *J. Phys. Chem. B* **2003**, *107*, 11307−11315.
(38) O'Regan, B. C.; Bakker, K.; Kroeze, J.; Smit, H.; Sommeling, P.; Durrant, J. R. Measuring charge transport from transient photovoltage rise times. A new tool to investigate electron transport in nanoparticle films. *J. Phys. Chem. B* **2006**, *110*, 17155−17160.
(39) van de Lagemaat, J.; Frank, A. J. Nonthermalized electron transport in dye-sensitized nanocrystalline TiO_2 films: Transient photocurrent and random-walk modeling studies. *J. Phys. Chem. B* **2001**, *105*, 11194−11205.
(40) Wang, X.; Karanjit, S.; Zhang, L.; Fong, H.; Qiao, Q.; Zhu, Z. Transient photocurrent and photovoltage studies on charge transport in dye-sensitized solar cells made from the composites of TiO_2 nanofibers and nanoparticles. *Appl. Phys. Lett.* **2011**, *98*, 082114.
(41) Nazeeruddin, M. K.; Fantacci, S.; Selloni, A.; Viscardi, G.; Liska, P.; Ito, S.; Takeru, B.; Grätzel, M. Combined experimental and DFT-TDDFT computational study of photoelectrochemical cell ruthenium sensitizers. *J. Am. Chem. Soc.* **2005**, *127*, 16835−16847.
(42) Nazeeruddin, M. K.; Zakeerruddin, S. M.; Humphry-Baker, R.; Jirousek, M.; Liska, P.; Vlachopoulos, N.; S, V.; Fischer, C. H.; Grätzel, M. Acid -base equilibria of (2,2′-Bipyridyl-4,4′-dicarboxylic acid)-ruthenium(II) complexes and the effect of protonation on charge-transfer sensitization of nanocrystalline titania. *Inorg. Chem.* **1999**, *38*, 6298−6305.
(43) Dell'Orto, E.; Raimondo, L.; Sassella, A.; Abbotto, A. Dye-sensitized solar cells: Spectroscopic evaluation of dye loading on TiO_2. *J. Mater. Chem.* **2012**, *22*, 11364−11369.
(44) Campbell, W. M.; J, K. W.; Wagner, P.; Wagner, K.; Walsh, P. J.; Gordon, K. C.; Schmidt-Mende, L.; Nazeeruddin, M. K.; Wang, Q.; Grätzel, M.; Officer, D. L. Highly efficient porphyrin sensitizers for dye-sensitized solar cells. *J. Phys. Chem. C* **2007**, *111*, 1760−1762.